EphA4 Misexpression Alters Tonotopic Projections in the Auditory Brainstem

Kelly J. Huffman,[1] Karina S. Cramer[2]

[1] Department of Psychology, University of California, Riverside, California 92521

[2] Department of Neurobiology and Behavior, University of California, Irvine, California 92697

Received 16 March 2007; accepted 3 May 2007

ABSTRACT: **Auditory pathways contain orderly representations of frequency selectivity, which begin at the cochlea and are transmitted to the brainstem via topographically ordered axonal pathways. The mechanisms that establish these tonotopic maps are not known. Eph receptor tyrosine kinases and their ligands, the ephrins, have a demonstrated role in establishing topographic projections elsewhere in the brain, including the visual pathway. Here, we have examined the function of these proteins in the formation of auditory frequency maps. In birds, the first central auditory nucleus, n. magnocellularis (NM), projects tonotopically to n. laminaris (NL) on both sides of the brain. We previously showed that the Eph receptor EphA4 is expressed in a tonotopic gradient in the chick NL, with higher frequency regions showing greater expression than lower frequency regions. Here we misexpressed EphA4 in the developing auditory brainstem from embryonic day 2 (E2) through E10, when NM axons make synaptic contact with NL. We then evaluated topography along the frequency axis using both anterograde and retrograde labeling in both the ipsilateral and contralateral NM-NL pathways. We found that after misexpression, NM regions project to a significantly broader proportion of NL than in control embryos, and that both the ipsilateral map and the contralateral map show this increased divergence. These results support a role for EphA4 in establishing tonotopic projections in the auditory system, and further suggest a general role for Eph family proteins in establishing topographic maps in the nervous system.** © 2007 Wiley Periodicals, Inc. Develop Neurobiol 67: 1655–1668, 2007

Keywords: **Eph receptor; ephrin; tonotopy; topography; nucleus laminaris; nucleus magnocellularis**

INTRODUCTION

Sensory pathways of the nervous system are generally organized topographically, so that neighboring areas of the sensory epithelium contact neighboring areas in the brain. This topography is often preserved at progressively higher levels of processing. The development of these topographic projections may involve activity-dependent refinement of initial projections, but often a significant level of topography is present at the outset, during development of synaptic connections (Friauf and Lohmann, 1999; Debski and Cline, 2002). This initial topography arises as a consequence of coordinated axon guidance signals (McLaughlin and O'Leary, 2005). While the nature of these molecular cues has been described in some areas of the nervous system, very little is known about the mechanisms that form topographic connections in auditory pathways.

In the auditory system, projections from the spiral ganglion to the cochlear nucleus have a significant degree of topography early in development in mammals and birds, with some subsequent refinement (Snyder and Leake, 1997; Leake et al., 2002; Molea

Correspondence to: K.S. Cramer (cramerk@uci.edu).

Contract grant sponsor: NIH NIDCD; contract grant number: 005771.

Contract grant sponsor: NIH NINDS; contract grant number: 050142.

Published online 18 June 2007 in Wiley InterScience (www.interscience.wiley.com).
DOI 10.1002/dneu.20535

and Rubel, 2003). Information from the cochlea is transmitted to the auditory brainstem via cochlear ganglion cells whose axons enter the brainstem through the VIIIth nerve (Rubel and Fritzsch, 2002). These connections synapse onto nucleus magnocellularis (NM) in a topographic manner (Rubel and Parks, 1975; Lippe and Rubel, 1985). This topography preserves the ordering of frequency selectivity first evident in the cochlea (Ryals and Rubel, 1982) and is referred to as tonotopy. NM neurons branch and project bilaterally to nucleus laminaris (NL). The ipsilateral branch contacts dorsal NL dendrites while the contralateral branch contacts ventral NL dendrites, and both of these projections are tonotopically organized. The topographic axis for both NM and NL extends from a rostromedial position, where high frequency sounds are represented, to caudolateral, where lower frequency sounds are encoded (Rubel and Parks, 1975). Each NL thus receives a tonotopic ipsilateral and contralateral projection from NM, and these frequency maps are in register. This circuitry facilitates sound localization using interaural time differences at each frequency.

In this study we tested the role of Eph protein signaling in the formation of topography in the NM-NL projection. Eph proteins, including Eph receptor tyrosine kinases and their ligands, the ephrins, have important roles in axon guidance and are known to be required for the formation of topography in the visual system. The Eph proteins include the EphA and EphB subclasses of Eph proteins, which bind ephrin-A and ephrin-B ligands, respectively. Two exceptions to this general rule are that EphA4 binds ephrin-B2 (Gale et al., 1996) and EphB2 binds ephrin-A5 (Himanen et al., 2004). As both ligands and receptors are associated with membranes, Eph/ephrin signaling mediates cell–cell interactions, which can be attractive or repulsive (reviewed in Pasquale, 2005), even within a single pathway (Hansen et al., 2004). Moreover, Eph receptors and ephrins can signal in both forward and reverse directions (Henkemeyer et al., 1996; Holland et al., 1996; Bruckner et al., 1997; Knoll and Drescher, 2002; Kullander and Klein, 2002). A consequence of this bidirectional signaling is that both ephrins and Eph receptors can function as axon guidance molecules.

Several Eph proteins are expressed in the auditory brainstem during development (Cramer et al., 2000b, 2002; Person et al., 2004; Cramer, 2005). The Eph receptor EphA4 is strongly expressed in the dorsal neuropil and in the cell bodies of NL at chick embryonic day 10 (E10), when synaptic connections form. Misexpression of EphA4 disrupts the segregation of ipsilateral and contralateral projections to dorsal *versus* ventral dendrites of NL (Cramer et al., 2004), suggesting a role for EphA4 in the developmental segregation of this circuit, which facilitates sound localization (Agmon-Snir et al., 1998). Whether or not EphA4 plays a similar developmental role in the formation of frequency maps in NL has not previously been determined. Within the dorsal neuropil of NL, at E10-11 there is a gradient of EphA4 expression, such that there is stronger expression in the rostromedial area of NL, which contains cells selective for high frequencies. This expression decreases in a gradient toward the caudolateral, low frequency region of NL (Person et al., 2004). These data suggest that EphA4, in addition to its role in segregating ipsilateral and contralateral inputs, may also play a significant role in the tonotopic ordering of connections.

To test this possibility, we misexpressed EphA4 *in ovo* in the developing auditory brainstem nuclei, and subsequently assessed the precision of the topography using *in vitro* dye labeling. We found that projections from NM to NL were significantly broader after EphA4 misexpression as compared to controls. Results from these experiments provide the first demonstration that Eph protein signaling functions to establish topography in the auditory system. These findings support a general role for Eph proteins in the production of topographic sensory maps.

MATERIALS AND METHODS

Plasmids

To transfect embryos using *in ovo* electroporation, we cloned full-length EphA4 into the pCAX plasmid vector. EphA4 was excised from the pcDNA3 vector at flanking *Eco*RI sites; it was then inserted into the pCAX plasmid vector at the *Eco*RI site, downstream of the β-actin promotor. Correct orientation of the insert was verified using HindIII. Embryonic transfection with EphA4 in pCAX greatly increases EphA4 levels in developing tissue, as demonstrated by immunohistochemistry (Cramer et al., 2004; Eberhart et al., 2004). For control samples, a pCAX-EGFP vector alone was electroporated into the tissue. In some control cases, no vector was electroporated to verify that pCAX-EGFP did not have an effect on topographic patterning.

In Ovo Electroporation

Fertilized eggs were set in a rotating 37°C incubator. We performed electroporation at embryonic day 2 (E2) because the locations of precursors for NM and NL are known at this age (Cramer et al., 2000a), and because electroporation at this age results in sustained transfection at E10 (Cramer et al., 2004, 2006), when NM and NL are distinct nuclei

and after NM-NL connections have formed (Saunders et al., 1973; Jackson et al., 1982; Young and Rubel, 1983; Momose-Sato et al., 2006). At E2, eggs were removed from the incubator, turned on their sides, and tape was placed on the lateral portion of the eggshell. A small amount of albumin was removed using a sterile 18-gauge hypodermic needle, and a round window was cut in the taped area. Using a 36-gauge hypodermic needle, an India ink solution (30% in sterile phosphate buffered saline, PBS) was injected beneath the embryo to provide contrast. Using a fine tungsten needle, a small opening was made in the roof plate of the embryo, at the level of rhomberes 5–6 (r5–r6). Sterile PBS (<5 μL) was placed on the neural tube opening. Plasmid DNA colored with a small amount of Fast Green dye was injected into the small neural tube opening using a fine glass pipette attached to a Picospritzer, and two to six injections of 50 ms duration were administered at a pressure of 15–20 psi, filling the neural tube at this rostrocaudal level. A BTX 830 electroporator connected to two tungsten electrodes was used for electroporation. One electrode was placed inside the opened neural tube, at the level of r5. The other electrode was placed outside the embryo, close to the lateral surface near r5. The separation between the two electrodes was about 200 μm. Electroporation in this region resulted in transfection that was extensive in, but not limited to, auditory brainstem nuclei. Between 5 and 10 six-pulse trains, at a voltage of 25–50 mV and 100 ms ISI, were delivered. In half of the trains, the negative electrode was inside the neural tube and the positive electrode was outside the embryo; the polarity was reversed for the remaining pulse trains. The eggshell window was closed and sealed with tape, and the egg was placed in a stationary humid incubator at 37°C for 8 days.

In Vitro Axon Labeling

On E10, chick embryos were removed from the eggshell and the brainstem was quickly dissected and placed in an oxygenated (95% O2/5% CO2) Tyrode's solution (8.12 g/L NaCl, 0.22 g/L KCl, 1.43 g/L $NaHCO_3$, 0.2 g/L $MgCl_2$, 0.333g/L $CaCl_2$, and 22 g/L dextrose). EGFP fluorescence was assessed in whole brainstems using a fluorescence stereomicroscope (Fig. 1), and tissue transfected in the region of the brainstem containing auditory nuclei was used for *in vitro* labeling. Methods used here are adapted from previously described protocols to label NM axons during development and after alteration of EphA4 levels in brainstem tissue (Young and Rubel, 1986; Cramer et al., 2004, 2006; Burger et al., 2005). Small unilateral injections of rhodamine dextran amine (RDA; MW = 3000; Molecular Probes) were placed in NM and NL using a Picospritzer. Injections into NM produced anterograde labeling, while injections into NL produced retrograde labeling. RDA was used in a 6.25% solution containing 0.4% Triton X-100 in PBS. Injections were made in a rostral, middle, or caudal location along the rostrocaudal axis of the brainstem [Fig. 1(A,B)]. We attempted to restrict each injection to no more than 1/3 to 1/2 of the total rostrocaudal length of the nucleus. A small current was passed through the tissue using electroporation to aid in dye uptake for retrograde labeling (Burger et al., 2005). Next, the brainstem was placed in a chamber filled with oxygenated Tyrode's solution for 2–5 h to allow RDA transport. The tissue was fixed for 1 h in 4% paraformaldehyde in PBS (pH = 7.4) at room temperature on a shaker. The tissue was washed in PBS and cryoprotected overnight in 30% sucrose in PBS. Tissue was embedded in OCT, frozen, and sectioned on a cryostat in the coronal plane into 16 μm sections. One series of sections was coverslipped with Glycergel for fluorescent visualization, one series was counterstained for bisbenzimide, and in some cases a third series was used for immunostaining. The bisbenzimide sections were used to anatomically define brainstem nuclear boundaries [Fig. 2(A)], fluorescent sections were used to evaluate transfection [Fig. 2(B)] and connections patterns, and immunostaining was used to detect the presence of exogenous EphA4 (see Cramer et. al, 2004). EphA4 was observed using immunohistochemistry or immunofluorescence using a secondary antibody conjugated to Alexa 594 (Molecular Probes, Eugene, OR).

Data Analysis

Brainstems were included in our analysis if auditory nuclei were transfected, if the RDA injection site and the surrounding dye uptake region extended to no more than half the total length of the nucleus injected, and if retrograde and/or anterograde transport successfully labeled cell bodies in NM or labeled axon terminations at NL. Samples were excluded if the injected dye extended through the entire rostrocaudal extent of the nucleus; if there was insufficient transport of dye; or if there was no transfection. For each condition, three to eight samples met the criteria; a total of 44 samples were included in the analysis. Slides were coded and scored blind to treatment group. For each section we noted the presence of EGFP in NL or NM or both, presence of injection site and extent of dye uptake region, presence of crossing fibers (to the contralateral side), and the presence of axon terminals at the NL neuropil or retrogradely labeled cells in NM. The tonotopic axis of NM and NL is rostromedial (high frequency) to caudolateral (low frequency), with the axis positioned about 30° with respect to the sagittal plane (Rubel and Parks, 1975). We thus used the rostrocaudal axis as a reasonable estimate of position along the tonotopic axis. We measured the rostrocaudal dimensions of the nuclei, extent of the injection site and dye uptake region, and the rostrocaudal extent of anterograde and retrograde labeling between the nuclei, both ipsilaterally and contralaterally. We used the following quantitative measurements of labeling so that experimental and control groups could be compared:

For anterogradely labeled brainstems, the proportion of NM injected with RDA was defined as:

1. $pNM_i = NM_{inj}/NM$, where NM_{inj}, the number of sections containing injected RDA within NM; NM, the total number of sections containing NM.

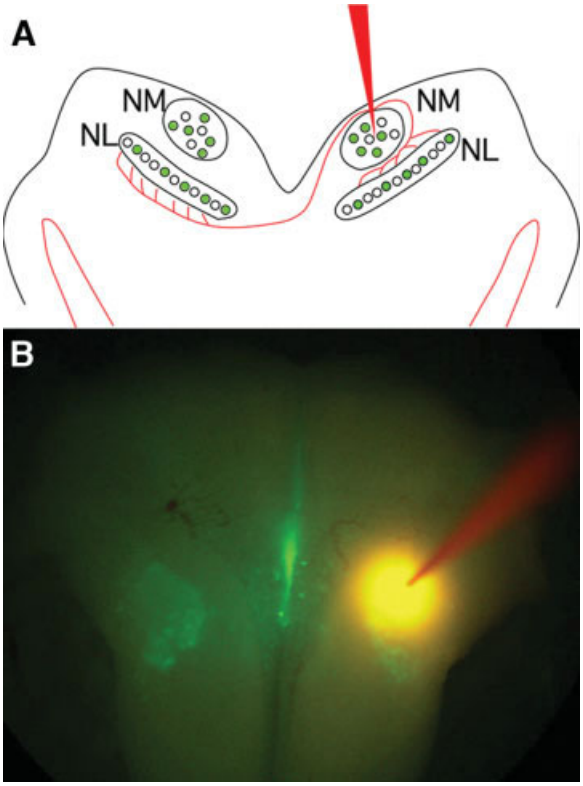

The proportion of NL anterogradely labeled with RDA was defined as

2. $pNL_a = NL_{ant}/NL$, where NL_{ant}, the number of sections containing RDA labeled axons in NL; NL, the total number of sections containing NL.

Figure 1 A: A drawing of a coronal section, with dorsal up, through a chick brainstem at embryonic day 10 (E10). The auditory brainstem nuclei n. magnocellularis (NM) and n. laminaris (NL) are outlined, and small circles within the nuclei represent cell bodies. The cell bodies labeled green represent those tranfected with EGFP. The red pipette indicates the position of an RDA injection, and the red lines represent labeled axons where the dye has transported anterogradely to the dorsal neuropil of NL ipsilaterally, and the ventral neuropil of NL contralaterally. This drawing illustrates the geometry of our labeling methods and demonstrates the precision of connections from NM to NL. B: A photomicrograph of a whole, dissected chick E10 brainstem, from a dorsal view with rostral up, that has been transfected with EGFP at E2. Auditory nuclei and midline structures were transfected (green). The red pipette and injection site shows the position and size of a rostral NM injection of RDA.

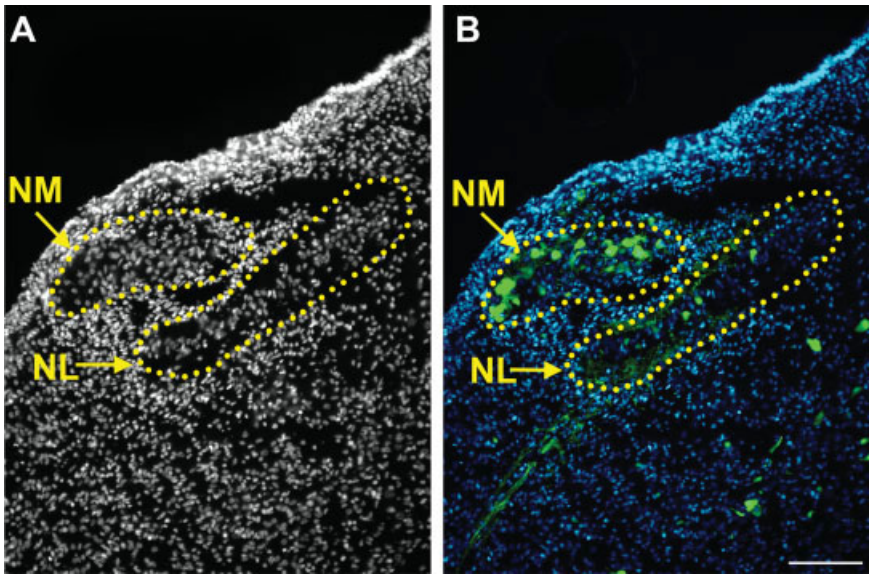

Figure 2 A: A gray-scale photomicrograph of the right side of a coronal section through the chick E10 brainstem. This section has been stained with bisbenzimide to illuminate the position and boundaries of NM and NL (oulined in yellow). Dorsal is up and medial is to the left. B: A color photomicrograph of the right brainstem shown in A. Cell nuclei are labeled blue with bisbenzimide. The green labeled cells, along with their axons, were transfected with EGFP control plasmid. Transfected cells are evident in both NM and NL (outlined in yellow) as well as elsewhere in the brainstem. Dorsal is up and medial is to the left. Scale bar for both panels, 100 μm.

As a measure of the divergence in the NM-NL projection, we used the ratio

3. $R_{Ant} = pNM_i/pNL_a$

Thus, a value greater than one indicates that a given fraction of NM projects to a narrower fraction of NL. A smaller value for R_{Ant} indicates greater divergence in the projection from NM to NL, i.e., that a small region of NM projects more broadly across the tonotopic axis of NL.

For brainstems with retrograde labeling, the proportion of NL injected with RDA was defined as

4. $pNL_i = NL_{inj}/NL$, where NL_{inj}, the number of sections containing injected RDA in NL; NL, the total number of sections containing NL.

The proportion of NM retrogradely labeled with RDA was defined as

5. $pNM_r = NM_{ret}/NM$, where NM_{ret}, the number of sections containing RDA labeled neurons in NM; NM, the total number of sections containing NM.

As a measure of the convergence in the NM-NL projection, we used the ratio

6. $R_{Ret} = pNL_i/pNM_r$

For retrograde labeling, a smaller value for R_{Ret} indicates greater convergence in the projection from NM to NL, i.e., that a small region of NL receives innervation from a broad area of NM. Values greater than one indicate that a given region of NL receives input from a smaller relative region of NM.

For each labeled embryo, we computed R_{Ant} or R_{Ret} as appropriate for the labeling in each brainstem. The mean R_{Ant} or R_{Ret} was computed for each group, with ipsilateral and contralateral labeling considered separately. Analysis of variance (ANOVA) and *t*-tests were performed to test for differences between control (EGFP alone or untransfected) and experimental (EphA4/EGFP) cases. All digital photography was done using a Zeiss Fluorescent Axioscope and a Zeiss Axiocam connected to an Apple computer running Openlab software.

RESULTS

NM-NL Projections in Control Embryos

Untransfected control embryos and control-transfected animals receiving pCAX-EGFP were both included in the analysis. For anterograde neuronal tracing, a limited region of NM was injected, and after dye transport the proportion of NM sections containing the injection site was compared to the proportion of NL sections containing anterogradely labeled axons using the ratio R_{Ant} (see Materials and Methods). The mean ratio for untransfected controls assessed with anterograde contralateral labeling was 0.96 ± 0.10 (SEM; $n = 3$). A representative example is shown in Figure 3. Here and in subsequent figures showing contralateral labeling we show a rostral to caudal sampling of sections with fluorescent labeling and bisbenzimide counterstain to show nuclear boundaries (outlined in yellow). The left column highlights the extent of the injection site on the left side, and the right column shows the resulting anterograde labeling on the right side. An injection was placed in rostral NM, and the proportion of NM containing the dye uptake region, pNM_i, was 0.47 [Fig. 3(A–C)]. The center of the injection site is noted with an asterisk [Fig. 3(B)], and regions of auditory nuclei that took up dye for transport are highlighted with bold dotted lines. This area of NM projected contralaterally to the ventral neuropil of NL. These projections spanned the rostral region of NL, with $pNL_a = 0.5$ [Fig. 3(A'–C')]. In this control case, the ratio was thus 0.94. As expected, NM axons in this control example project contralaterally to ventral NL, and do not cross the NL cell body line [Fig. 3(A'–C')]. Results from these untransfected embryos did not differ from EGFP control cases, in which R_{Ant} was 1.23 ± 0.26 ($n = 3$; $p > 0.2$, *t*-test).

When all untransfected and EGFP controls were compared using ANOVA, we found that the groups did not differ ($p > 0.45$). Untransfected and EGFP control experiments demonstrate that, as expected, the electroporation procedure itself has no effect on topography. Because of the similarity of values for both control groups, we grouped together untransfected and EGFP controls for each type of labeling in subsequent analyses. For contralateral labeling, the mean control R_{Ret} was 0.86 ± 0.07 ($n = 6$) and the mean control R_{Ant} was 1.10 ± 0.14 ($n = 6$). For ipsilateral labeling, the mean control R_{Ret} was 1.02 ± 0.21 ($n = 3$) and the mean control R_{Ant} was 0.90 ± 0.10 ($n = 3$). A representative example of retrograde contralateral labeling in an EGFP control brainstem is shown in Figure 4. In this case, an injection was placed in rostral NL, and was measured to span the rostral 54% of NL, so that $pNL_i = 0.54$ [Fig. 4(A–C)]. The NL injection site was centered in the section shown in Figure 4(B) (asterisk) and dye uptake extended through sections shown in Figure 4(A–C) (bold dotted lines). The proportion of retrogradely labeled cells in contralateral NM was 0.53 in the rostral region of NM [Fig. 4(A'–C')]. In this case the ratio for retrograde labeling, R_{Ret}, was 1.02. Our retrograde contralateral labeling data were similar to previously published results for E18 embryos (Burger et al., 2005), suggesting that the topography of NM-NL projections is largely established by E10.

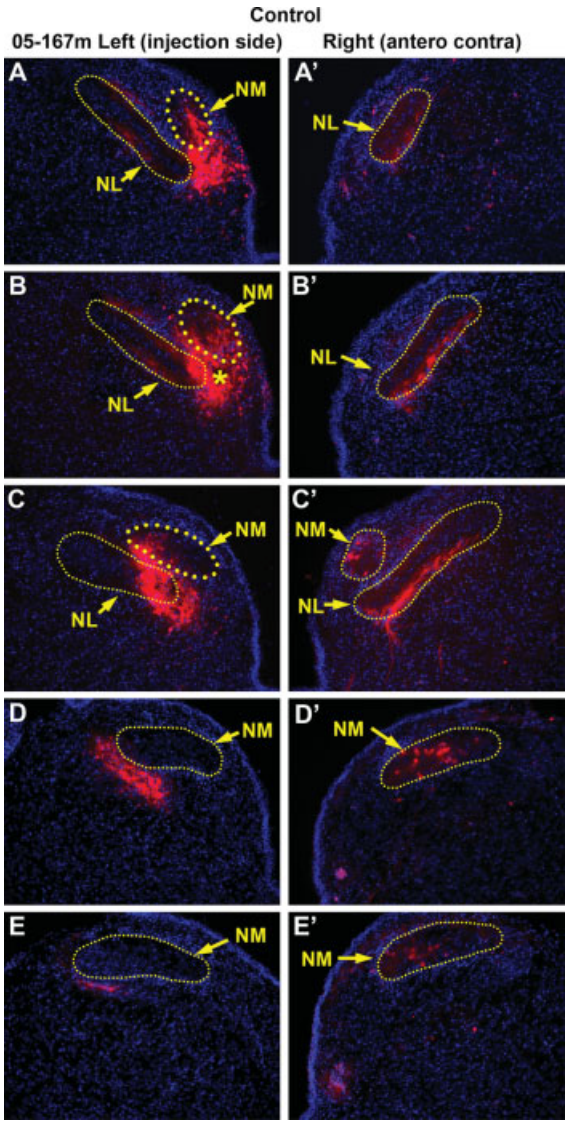

Figure 3 A rostral to caudal progression of a subset of coronal sections from a control E10 brainstem from case 05-167m, an untransfected control, with anterograde labeling of the contralateral projection. A-E: sections through the left side of the brainstem demonstrating the position of the RDA injection site in NM, the center of which is located in B (denoted by a yellow asterisk). NM within dye uptake region is outlined by bold dotted lines in A-C. In this case, the RDA is in rostral NM, and encompasses 0.47 of the rostrocaudal length of NM. A'–E': Sections through the right side of the brainstem showing anterograde contralateral projections from NM (left column) to the ventral neuropil of NL on the right. The rostrocaudal length of NL had a proportion of 0.5 that received input from the contralateral NM injection. Note that labeled axons can be seen on the ventral neuropil of NL in A'–C', and they do not cross into the dorsal neuropil. In this case the ratio R_{Ant}, which denotes the proportion of NM injected divided by the proportion of NL labeled, was 0.94. Using the blue nuclear stain bisbenzimide as a guide, NM and NL have been outlined in yellow in all panels. Scale bar, 100 μm.

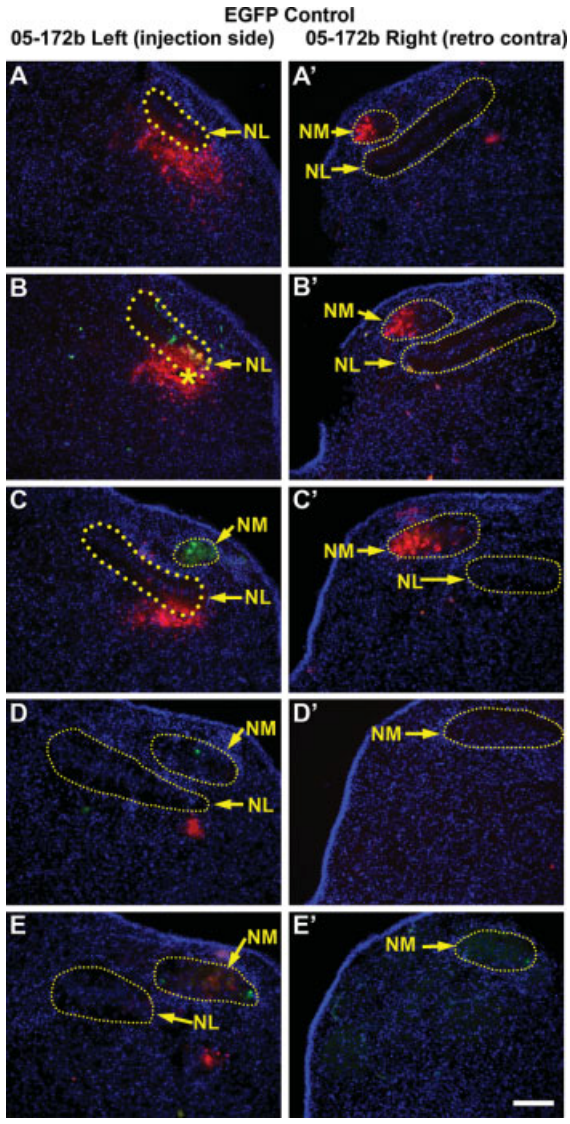

Figure 4 A rostral to caudal progression of coronal sections from a control E10 brainstem. In this case (05-172b), the E2 embryo was electroporated with pCAX-EGFP, *in ovo*, for control. The green EGFP labeled cells are those transfected with pCAX-EGFP. Contralateral projections were labeled retrogradely with RDA. A–E: sections through the left side of the brainstem demonstrating the position of the RDA injection site in NL, centered in the section shown in B (asterisk) with dye uptake extending from A to C. In this case, the injection site is near rostral NL, and uptake extends to 0.54 of the rostrocaudal length of NL. A'–E': Sections through the right side of the brainstem showing retrograde contralateral input (labeled cells) from NM projecting to the NL dye uptake region shown in the left column (A–C). The portion of NL (0.54) containing injected RDA received input from 0.53 of the rostrocaudal length of the contralateral NM (A'–E'). Note that retrogradely labeled cells can be seen in NM in A'–C'. The ratio R_{Ret} is defined as the proportion of NL injected divided by the proportion of NM with retrogradely labeled cells. In this representative example, R_{Ret} was 1.02. Scale bar, 100 μm.

In these control experiments, there was no significant difference between ipsilateral and contralateral projections when assessed using anterograde labeling ($p > 0.15$, *t*-test; $n = 3$ ipsilateral, $n = 6$ contralateral) or retrograde labeling ($p > 0.2$; $n = 3$ ipsilateral, $n = 6$ contralateral). This comparison shows that in normal embryos, assessed at this level of resolution of our labeling methods, topography is similar on both sides and is mature at E10.

Misexpression of EphA4 *In Ovo* Disrupts Topographic Patterning

E2 embryos were electroporated in the hindbrain with EphA4-pCAX and EGFP-pCAX to transfect the developing auditory brainstem neurons and test the hypothesis that EphA4 is involved in topographic patterning. Eight days after transfection (at E10), we examined brainstem explants for EGFP, and RDA labeling was used in successfully transfected embryos to assess the topographic connections between NM and NL. Anterograde and retrograde labeling were both used, and both the ipsilateral and contralateral projections were studied. In each of these groups 5–8 embryos were included in the analysis. Representative examples of each condition are represented in Figures 5–7.

In the analysis of anterograde contralateral neuronal tracing in embryos with EphA4 misexpression ($n = 7$; representative example shown in Fig. 5), EGFP positive cells were observed in both NL and NM [see green cells in Fig. 5(A–E')]. In the example shown in Figure 5, an injection of RDA was placed in the caudal region of NM, and the dye uptake expanded into the caudal half (0.50) of NM [Fig. 5(D,E)]. This injection site location in NM [Fig. 5(D,E) bold dotted lines, asterisk indicates center of injection site] resulted in RDA labeled contralateral axons in the ventral neuropil of NL. These projections labeled the entire rostrocaudal extent of NL [Fig. 5(A'–E')]. For this embryo, R_{Ant} was 0.50. Some NM axon branches can be seen growing across the cell body line in contralateral NL and terminating inappropriately in dorsal NL, consistent with our previous study [Cramer et al., 2004; Fig. 5(A'–C')]. For anterograde contralateral labeling of EphA4 transfected brainstems, the mean value R_{Ant} was 0.47 ± 0.05 ($n = 7$), which was significantly less than controls (1.10 ± 0.14; $n = 6$) that were also assessed with anterograde contralateral labeling ($p < 0.0005$). This result shows that EphA4 transfection results in a smaller NM/NL ratio, which indicates a broader extent of NL contacted by a given region of NM.

EphA4 electroporation also produced broadening of projections along the topographic axis when assessed using retrograde contralateral labeling ($n = 8$ embryos); a typical example is shown in Figure 6. Here EGFP positive cells were observed in both NL and NM [Fig. 6(A–E')]. The green label in the NL neuropil likely represents EGFP-expressing NM axons. An injection of RDA was placed in a region of the brainstem containing caudal NL, and the proportion of NL in the dye uptake region was 0.33 [Fig. 6(C,D)]. The NL injection was centered on sections shown in Figure 6(C,D) (asterisks). Retrograde labeling of neurons in contralateral NM show that this region of NL received inputs from the contralateral caudal 63% of NM [Fig. 6(A'–E')]. In this electroporated EphA4 case, R_{Ret} was 0.52. The mean value of R_{Ret} for all retrograde contralateral labeling in EphA4 transfected brainstems was 0.51 ± 0.05 ($n = 8$), which was significantly less than controls assessed using the same labeling method ($p < 0.005$). This result shows that EphA4 transfection results in a smaller NL/NM ratio, which indicates that a broader region of NM converges upon a given limited region of NL.

In addition to these contralateral projections, ipsilateral projections from NM to NL were also significantly broadened after overexpression of EphA4. Retrograde ipsilateral labeling in a brainstem following EphA4 misexpression ($n = 6$ embryos) is illustrated in Figure 7. In this representative example, RDA was placed in the rostral region of NL, and the dye uptake included 0.35 of NL [Fig. 7(A)]. This dye placement in NL resulted in retrogradely labeled cells in ipsilateral NM, from the ipsilateral rostral 0.50 of NM [Fig. 7(B–D)]. In this electroporated EphA4 case, the ratio R_{Ret} was 0.7. The mean R_{Ret} for ipsilateral projections in EphA4 treated animals was 0.72 ± 0.03 ($n = 6$). This value is signifcantly different from retrogradely labeled ipsilateral projections in controls ($p < 0.05$), demonstrating significantly broader ipsilateral NM-NL projections following EphA4 misexpression.

A similar result was observed using *anterograde* labeling of ipsilateral projections ($n = 5$ embryos). In the EphA4 misexpression example shown in Figure 7, an injection of RDA was placed near the rostral region of NM with dye uptake extending to a proportion of 0.32 of NM sections [Fig. 7(I,J)]. This injection resulted in anterograde labeling of ipsilateral axons to the dorsal neuropil of NL. The proportion of NL with labeled axons was 0.62 of NL [Fig. 7(F–I)]. In this example R_{Ant} was 0.52. In addition, some axons from NM extend across the NL cell body line into the ventral neuropil region [Fig. 7(G–I)] consistent with previous findings (Cramer et al., 2004). The

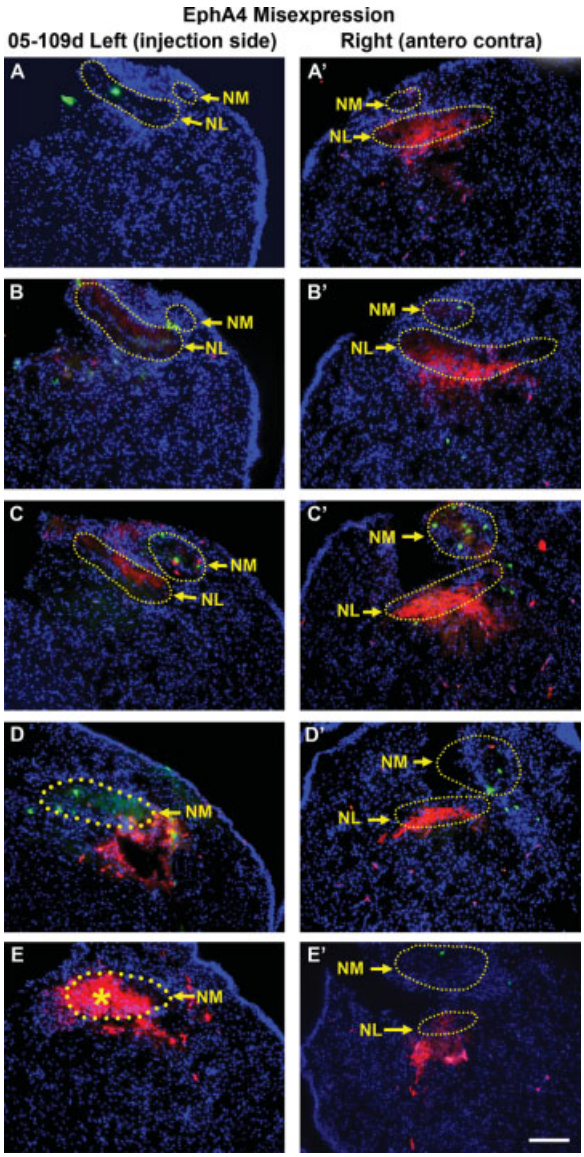

Figure 5 EphA4 misexpression reduces the ratio R_{Ant}, reflecting a broadening of the NM-NL projection. A representative case is shown in a rostral to caudal series of selected coronal sections from an E10 brainstem in which the contralateral projection was assessed with anterograde labeling. In this case (05-109d), the E2 embryo was electroporated with EphA4 and EGFP, *in ovo*, in order to misexpress EphA4 in NL and/or NM. A–E: sections through the left side of the brainstem demonstrating the position of the RDA injection site in NM. The asterisk in E shows the center of the injection site, which extends through caudal NM in sections shown in D and E (bold dotted lines). The injection site extends to 0.5 of the rostrocaudal length of NM. A'–E': Sections through the right side of the brainstem showing anterograde contralateral projections from NM (left column) to the ventral neuropil of NL (right column). The entire rostrocaudal length of NL received input from the contralateral NM injection site. Note that labeled axons can be seen in all sections through NL. In this case the ratio R_{Ant} was 0.5. Scale bar, 100 μm.

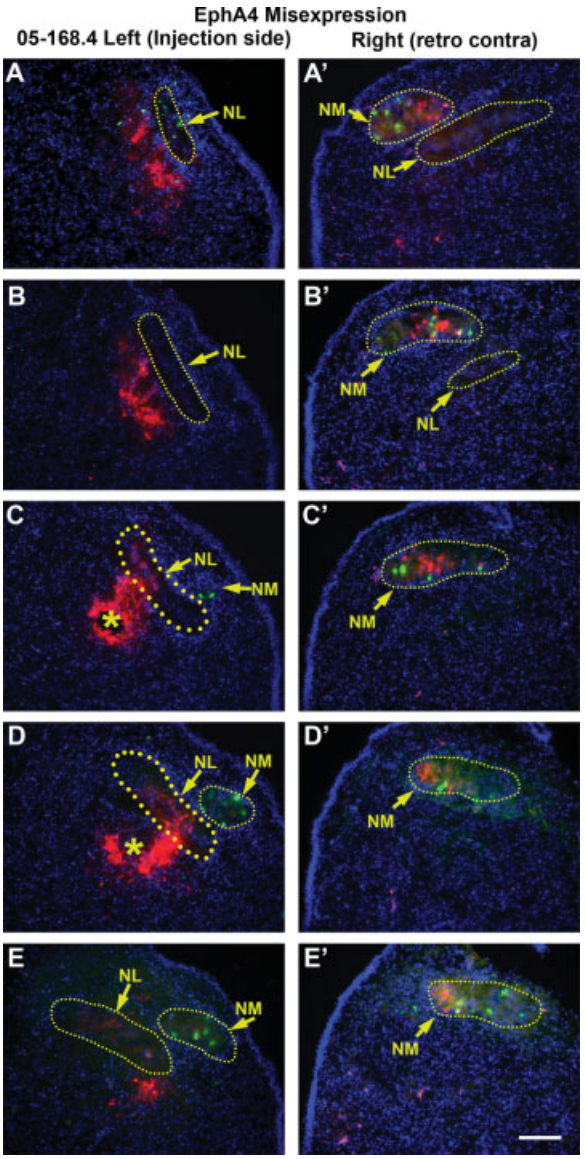

Figure 6 Retrograde labeling also shows a broader NM-NL contralateral projection (smaller R_{Ret}) after EphA4 misexpression. A–E: sections through the left side of the brainstem demonstrating the position of the RDA injection site ventral to NL, centered in C and D (asterisks). In this case, the dye uptake region encompasses 33% of the rostrocaudal length of NL (outlined in bold dotted lines). A'–E': Sections through the right side of the brainstem showing retrogradely labeled NM cells that project contralaterally to dye uptake region of NL. The caudalmost 0.33 of NL received input from 0.63 of the rostrocaudal length of the contralateral NM (A'–E'). Here R_{Ret} was 0.52. Scale bar, 100 μm.

mean R_{Ant} for anterogradely labeled ipsilateral projections was 0.58 $\pm$ 0.03 ($n = 5$), which differed significantly from controls with the same labeling method ($p < 0.05$). This result supports the conclu-

sion that ipsilateral projections are broadened after overexpression of EphA4.

The results of all the brainstems studied here are summarized in Figure 8. The anterograde labeling experiments, shown in the top graph, show a significantly lower R_{ant} for EphA4 treated animals than for controls, indicated by asterisks. The number of embryos used in each group is indicated above each bar. The difference is significant for both contralateral and ipsilateral NM-NL projections. The bottom graph shows results for retrograde labeling, in which R_{ret} is also significantly lower for EphA4 misexpression cases than for controls. Together, these results demonstrate that for both ipsilateral and contralateral NM-NL projections, the tonotopic map is broader after EphA4 misexpression than in control animals. This result is significant when assessed using anterograde labeling or retrograde labeling. The results from our EphA4 misexpression studies suggest that the gradient of EphA4 expression in NL limits the topographic spread of NM-NL projections along the tonotopic axis. Thus, EphA4 has a role in regulating the tonotopic specificity of these auditory brainstem pathways.

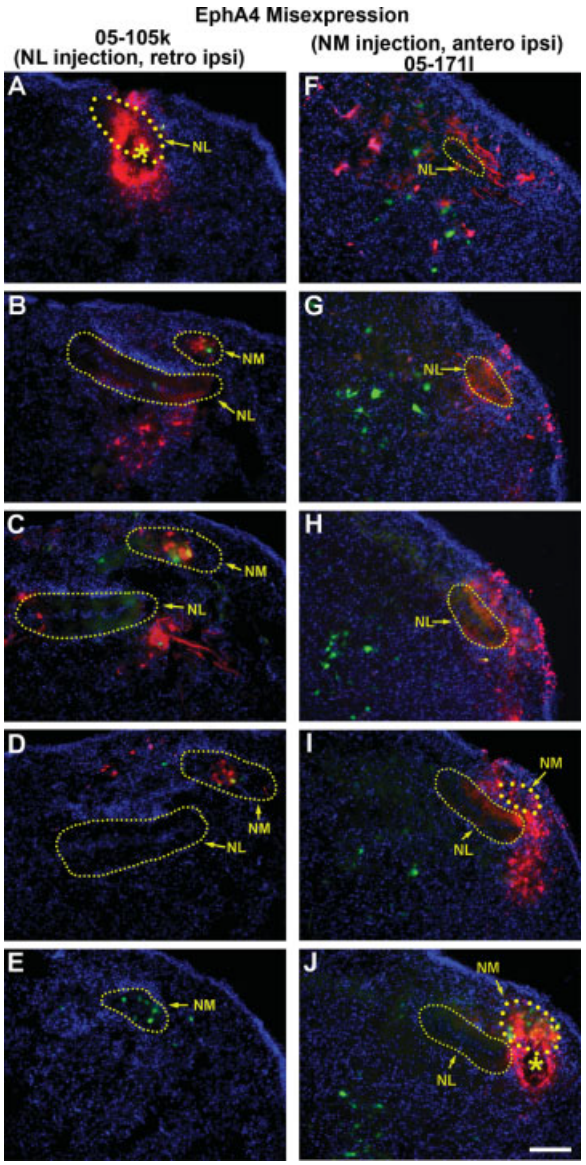

DISCUSSION

In this study we used anterograde and retrograde neuronal tracing to evaluate the extent of topography in the projection from NM to NL. We found that the projection along the frequency axis is topographically organized at E10, when the first synaptic connections form between NM and NL. Because EphA4 is expressed in a tonotopic gradient, we hypothesized that forced expression of EphA4 during development would disrupt the accuracy of the tonotopic map. Our neuroanatomical tracing studies after EphA4 misexpression support this hypothesis. We found that both the contralateral and ipsilateral projections were significantly broader after EphA4 misexpression than in controls. These data suggest that gradients of EphA4 expression in the developing auditory brainstem play a role in the formation of precisely ordered frequency maps.

Formation of Auditory Topographic Maps

We performed neuroanatomical dye tracing studies in control embryos to evaluate topography quantita-

Figure 7 EphA4 misexpression disrupts tonotopy of NM-NL ipsilateral projections. A–E: Retrograde labeling in an embryo (05-105k) treated with EphA4 misexpression and assessed with retrograde labeling. Sections through the left side of the brainstem demonstrate the position of the RDA injection site in NL, with a center in A (asterisk), and dye uptake in NL shown in bold dotted lines. The resulting retrogradely labeled cells in NM are seen on the same side (ipsilateral; B–D). In this case, the injection site is in rostral 0.35 of NL. Additionally, these sections show the extent of retrogradely labeled ipsilateral projections from NM (B–E). The injected region of NL received input from 0.5 of the rostrocaudal length of the ipsilateral NM; R_{Ret} was 0.7. F–J: Anterograde labeling of the ipsilateral NM-NL projection in another embryo (05-171l) with EphA4 misexpression. The position of the RDA injection site near NM is centered in the section shown in J (asterisk) and extends into NM in the sections shown in I and J (outlined in bold dotted lines), filling 0.32 of NM. The resulting anterogradely labeled axons on the dorsal neuropil of NL on the same side are shown in F–I and extend to 0.62 of NL; R_{Ant} was 0.52. Scale bar, 100 μm.

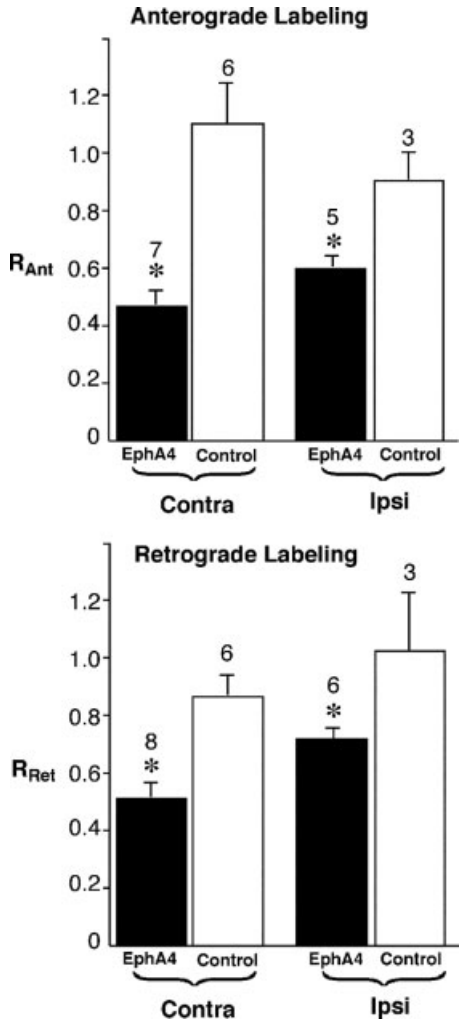

Figure 8 Summary of the results from this study. The total number of embryos used in each group is indicated above each bar. Top, anterograde labeling studies of contralateral and ipsilateral projections for EphA4 misexpression and control embryos. The ratio R_{ant}, defined as the proportion of NM injected: the proportion of NL labeled, was significantly lower (asterisk) than controls using the same labeling conditions, for both ipsilateral and contralateral projections. The decreased ratio signifies a broader spread of projections from NM to NL. Bottom, similar graph showing results from retrograde labeling studies. R_{ret} is significanly lower in EphA4 misexpression cases than in control embryos. Both methods show a broader spread of NM-NL projections in EphA4 misexpression cases than in controls.

tively. Our results suggest that precision in the tonotopic map from NM to NL is present from very early stages. The methods and results reported here are similar to those reported for E18 embryos (Burger et al., 2005), in which NL dye injections yielded retrograde contralateral labeling in NM. In that study, injections limited to circumscribed regions of the tonotopic axis of NL resulted in limited labeling of NM. Our ratios for control retrograde contralateral labeling were similar to those reported in that study, suggesting that there is little refinement of this projection between E10 and E18. That axonal projections are specified prior to the onset of neuronal activity suggests that axon guidance molecules play a major role in the formation of this topographic map, while activity-dependent mechanisms have a smaller role.

Our findings are consistent with data obtained in a previous study of individual NM axons (Young and Rubel, 1986), which showed that as early as E9 NM axon terminals were mostly in appropriate tonotopic NL locations in both ipsilateral and contralateral projections. While both projections had significant precision at early developmental time points, their study found that the contralateral projection is less precise and undergoes subsequent tonotopic refinement. In contrast, our data did not show a significant difference between these projections at E10. This discrepancy is likely attributable to differences in the anatomical approaches used, as single axon studies may have higher resolution and would reveal small differences. Moreover, we used the rostrocaudal axis as an estimate of frequency position to facilitate quantitative comparisons between treatment groups, but this estimate might reduce resolution in measurements of absolute levels of tonotopy.

In addition to the NM-NL projection, other auditory pathways may also have a high degree of precision in the initial projection. For example, topographic precision was observed in the spiral ganglion projection to the cochlear nucleus in cats, with a small degree of refinement in early stages of development (Snyder and Leake, 1997; Leake et al., 2002). Tonotopic projections in several regions of the auditory nervous system, both in the brainstem and higher areas, may rely more significantly on refinement of initial projections (Sanes and Takacs, 1993; Zhang et al., 2002; Kim and Kandler, 2003). However, the initial specificity in NM-NL projections suggests a substantial role for molecular cues, and this observation motivated our analysis of candidate molecules.

Eph Protein Interactions in the Auditory Brainstem

We focused our study on EphA4 because this protein is expressed in a frequency gradient in NL cell bodies and dorsal neuropil during the formation of synaptic connections (Person et al., 2004). In addition, we previously showed that EphA4 regulates the segregation

of ipsilateral and contralateral inputs from NM to NL (Cramer et al., 2004). In that study, focal electroporation revealed that EphA4 is most likely operating in a reverse signaling mode, in which Eph receptors signal through ephrins, and may attract NM axons. A likely binding partner for EphA4 is ephrin-B2, which is expressed on NM axons (Cramer et al., 2002, 2006). While ephrin-B2 appears to be expressed uniformly throughout NM, it is expressed in a tonotopic gradient in the glial margin ventral to NL (Person et al., 2004). These proteins may thus interact during establishment of the tonotopic NM-NL projection.

Several other Eph proteins are expressed in the developing auditory brainstem circuitry (Cramer et al., 2002; Cramer, 2005). EphA4 might work in conjunction with these other family members to establish precise connections along the frequency axis. In addition, EphA4 may interact with the neurotrophin receptor TrkB, which is expressed only in ventral NL dendrites at a time when EphA4 is expressed only in dorsal dendrites (Cochran et al., 1999; Cramer et al., 2000b). While it is not clear whether TrkB is expressed in a tonotopic gradient, interactions between these protein families play a role in the maturation of retinotopic maps (Cohen-Cory and Fraser, 1995; McLaughlin and O'Leary, 2005). In NL, EphA4 asymmetry on the dorsal dendrites slightly precedes TrkB asymmetry during development. An intriguing possibility is that EphA4 and TrkB on dorsal and ventral NL dendrites, respectively, coordinate the registration of ipsilateral and contralateral NM-NL topography.

Eph Protein Mechanisms and Topographic Maps

Our interpretation of the role of Eph proteins in the NM-NL tonotopic map may be informed by our knowledge of the roles of these proteins in other pathways. In addition to visual pathways, Eph proteins have been shown to establish topography in several other systems, including the somatosensory cortex (Prakash et al., 2000; Vanderhaeghen et al., 2000; Dufour et al., 2003), the olfactory system (Zhang et al., 1996; St John et al., 2002; Cutforth et al., 2003), hippocampal projections (Gao et al., 1996, 1999; Yue et al., 2002), and motor projections to limb muscles (Feng et al., 2000; Helmbacher et al., 2000; Kania and Jessell, 2003; Eberhart et al., 2004). The role of Eph proteins in topographic map formation is best understood in the retinotectal pathway, in which mechanisms of Eph protein interactions have been characterized in considerable detail (reviewed in Mann et al., 2004; Lemke and Reber, 2005; McLaughlin and O'Leary, 2005). Opposing gradients of ephrin-A ligands in the tectum and EphA receptors in retinal ganglion cells mediate repulsive interactions that control axon branching and establish topography along the anteroposterior axis of the tectum in birds and superior colliculus in mammals (Cheng et al., 1995; Yates et al., 2001; Feldheim et al., 2004). Mapping depends on relative levels of Eph protein expression between neighboring regions (Brown et al., 2000; Reber et al., 2004; Lemke and Reber, 2005). In addition, ephrin-B ligands and EphB receptors promote retinotopic ordering along the dorsoventral axis (Braisted et al., 1997; Hindges et al., 2002; Mann et al., 2002; McLaughlin et al., 2003); ordering along this axis includes chemoattractive interactions and reverse signaling, and may require ephrin-A signaling as well (Feldheim et al., 2000).

In the auditory pathways described here, details of the protein interactions that establish topography have yet to be identified. However, while the gradient of EphA4 and role for EphA4 bears similarity to retinotectal map formation, some important observations suggest differences in signaling mechanisms. Our initial data here and in our previous study (Cramer et al., 2004) suggest that EphA4 signals in the reverse direction, and may promote attraction of NM axons. This map formation might thus be more similar to that of the dorsoventral retinotopic projection. In addition, as noted earlier, Eph protein expression gradients have not been identified in NM axons. Finally, there is not extensive overshoot and refinement of NM axons projecting to NL (Young and Rubel, 1986), as observed in the retinotectal map; however, the role of Eph proteins in auditory axon branching remains an important yet unanswered question.

Topographic registry is often preserved between brain areas as sensory information ascends the nervous system. How extensively do Eph proteins contribute to the formation of these neural maps? In the visual pathway, several higher areas show graded expression of Eph proteins (Marin et al., 2001), and ephrin-A ligands are necessary for topography in visual cortex (Cang et al., 2005). Eph proteins are expressed in several areas of the auditory pathway. In the VIIIth nerve, auditory axons express EphA4 in a low-to-high frequency gradient (Siddiqui and Cramer, 2005), and ephrin-A ligands show graded expression in the medial geniculate nucleus of the thalamus (Lyckman et al., 2001; Ellsworth et al., 2005). Functional studies are needed to elucidate the roles of these proteins throughout the auditory pathway. Moreover, Eph proteins may have several distinct roles within a pathway. In the NM-NL projection,

EphA4 regulates both tonotopic organization, as shown in this study, and the segregation of ipsilateral and contralateral inputs (Cramer et al., 2004). Interestingly, ephrins are important for both retinotopy and the segregation of eye-specific layers in the lateral geniculate nucleus (Huberman et al., 2005; Pfeiffenberger et al., 2005). Thus, multiple roles of Eph proteins might generally serve to facilitate coordination of several organizing features within a sensory projection. A limitation of our approach is that we have examined only gain-of-function with forced expression. This type of overexpression has previously been used to identify a role for Eph proteins in retinal patterning (Nakamoto et al., 1996; Dutting et al., 1999). Loss-of-function studies complement this approach. While the mouse lacks a structure homologous to NL, we have examined several auditory pathways in EphA4 mutant mice, and in preliminary studies we have found that this mutation disrupts organization of auditory brainstem pathways (Miko et al., submitted).

In conclusion, this report presents evidence demonstrating the role of EphA4 in the development of appropriate topographic connections in the auditory system. These results show that mechanisms involving the Eph family of molecules extend to the auditory system. Moreover, in this system activity-dependent mechanisms do not appear to have a major role in refinement. Studies on the formation of topography have thus far implicated several mechanisms, including a variety of Eph protein signaling modes. A rigorous examination of mechanisms in a broad range of systems will ultimately contribute to an understanding of the rules that govern map formation during the assembly of neural circuits.

The authors thank Dr. Ilona Miko for helpful comments on the manuscript and Shazia Siddiqui for technical assistance.

REFERENCES

Agmon-Snir H, Carr CE, Rinzel J. 1998. The role of dendrites in auditory coincidence detection. Nature 393:268–272.

Braisted JE, McLaughlin T, Wang HU, Friedman GC, Anderson DJ, O'Leary DD. 1997. Graded and lamina-specific distributions of ligands of EphB receptor tyrosine kinases in the developing retinotectal system. Dev Biol 191:14–28.

Brown A, Yates PA, Burrola P, Ortuno D, Vaidya A, Jessell TM, Pfaff SL, et al. 2000. Topographic mapping from the retina to the midbrain is controlled by relative but not absolute levels of EphA receptor signaling. Cell 102: 77–88.

Bruckner K, Pasquale EB, Klein R. 1997. Tyrosine phosphorylation of transmembrane ligands for Eph receptors. Science 275:1640–1643.

Burger RM, Cramer KS, Pfeiffer JD, Rubel EW. 2005. Avian superior olivary nucleus provides divergent inhibitory input to parallel auditory pathways. J Comp Neurol 481:6–18.

Cang J, Kaneko M, Yamada J, Woods G, Stryker MP, Feldheim DA. 2005. Ephrin-as guide the formation of functional maps in the visual cortex. Neuron 48:577–589.

Cheng HJ, Nakamoto M, Bergemann AD, Flanagan JG. 1995. Complementary gradients in expression and binding of ELF-1 and Mek4 in development of the topographic retinotectal projection map. Cell 82:371–381.

Cochran SL, Stone JS, Bermingham-McDonogh O, Akers SR, Lefcort F, Rubel EW. 1999. Ontogenetic expression of trk neurotrophin receptors in the chick auditory system. J Comp Neurol 413:271–288.

Cohen-Cory S, Fraser SE. 1995. Effects of brain-derived neurotrophic factor on optic axon branching and remodelling in vivo. Nature 378:192–196.

Cramer KS. 2005. Eph proteins and the assembly of auditory circuits. Hear Res 206:42–51.

Cramer KS, Bermingham-McDonogh O, Krull CE, Rubel EW. 2004. EphA4 signaling promotes axon segregation in the developing auditory system. Dev Biol 269:26–35.

Cramer KS, Cerretti DP, Siddiqui SA. 2006. EphB2 regulates axonal growth at the midline in the developing auditory brainstem. Dev Biol 295:76–89.

Cramer KS, Fraser SE, Rubel EW. 2000a. Embryonic origins of auditory brain-stem nuclei in the chick hindbrain. Dev Biol 224:138–151.

Cramer KS, Karam SD, Bothwell M, Cerretti DP, Pasquale EB, Rubel EW. 2002. Expression of EphB receptors and EphrinB ligands in the developing chick auditory brainstem. J Comp Neurol 452:51–64.

Cramer KS, Rosenberger MH, Frost DM, Cochran SL, Pasquale EB, Rubel EW. 2000b. Developmental regulation of EphA4 expression in the chick auditory brainstem. J Comp Neurol 426:270–278.

Cutforth T, Moring L, Mendelsohn M, Nemes A, Shah NM, Kim MM, Frisen J, et al. 2003. Axonal ephrin-As and odorant receptors: Coordinate determination of the olfactory sensory map. Cell 114:311–322.

Debski EA, Cline HT. 2002. Activity-dependent mapping in the retinotectal projection. Curr Opin Neurobiol 12:93–99.

Dufour A, Seibt J, Passante L, Depaepe V, Ciossek T, Frisen J, Kullander K, et al. 2003. Area specificity and topography of thalamocortical projections are controlled by *ephrin/Eph* genes. Neuron 39:453–465.

Dutting D, Handwerker C, Drescher U. 1999. Topographic targeting and pathfinding errors of retinal axons following overexpression of ephrinA ligands on retinal ganglion cell axons. Dev Biol 216:297–311.

Eberhart J, Barr J, O'Connell S, Flagg A, Swartz ME, Cramer KS, Tosney KW, et al. 2004. Ephrin-A5 exerts positive or inhibitory effects on distinct subsets of EphA4-positive motor neurons. J Neurosci 24:1070–1078.

Ellsworth CA, Lyckman AW, Feldheim DA, Flanagan JG, Sur M. 2005. Ephrin-A2 and -A5 influence patterning of normal and novel retinal projections to the thalamus: Conserved mapping mechanisms in visual and auditory thalamic targets. J Comp Neurol 488:140–151.

Feldheim DA, Kim YI, Bergemann AD, Frisen J, Barbacid M, Flanagan JG. 2000. Genetic analysis of ephrin-A2 and ephrin-A5 shows their requirement in multiple aspects of retinocollicular mapping. Neuron 25:563–574.

Feldheim DA, Nakamoto M, Osterfield M, Gale NW, DeChiara TM, Rohatgi R, Yancopoulos GD, et al. 2004. Loss-of-function analysis of EphA receptors in retinotectal mapping. J Neurosci 24:2542–2550.

Feng G, Laskowski MB, Feldheim DA, Wang H, Lewis R, Frisen J, Flanagan JG, et al. 2000. Roles for ephrins in positionally selective synaptogenesis between motor neurons and muscle fibers. Neuron 25:295–306.

Friauf E, Lohmann C. 1999. Development of auditory brainstem circuitry. Activity-dependent and activity-independent processes. Cell Tissue Res 297:187–195.

Gale NW, Holland SJ, Valenzuela DM, Flenniken A, Pan L, Ryan TE, Henkemeyer M, et al. 1996. Eph receptors and ligands comprise two major specificity subclasses and are reciprocally compartmentalized during embryogenesis. Neuron 17:9–19.

Gao PP, Yue Y, Cerretti DP, Dreyfus C, Zhou R. 1999. Ephrin-dependent growth and pruning of hippocampal axons. Proc Natl Acad Sci USA 96:4073–4077.

Gao PP, Zhang JH, Yokoyama M, Racey B, Dreyfus CF, Black IB, Zhou R. 1996. Regulation of topographic projection in the brain: Elf-1 in the hippocamposeptal system. Proc Natl Acad Sci USA 93:11161–11166.

Hansen MJ, Dallal GE, Flanagan JG. 2004. Retinal axon response to ephrin-as shows a graded, concentration-dependent transition from growth promotion to inhibition. Neuron 42:717–730.

Helmbacher F, Schneider-Maunoury S, Topilko P, Tiret L, Charnay P. 2000. Targeting of the EphA4 tyrosine kinase receptor affects dorsal/ventral pathfinding of limb motor axons. Development 127:3313–3324.

Henkemeyer M, Orioli D, Henderson JT, Saxton TM, Roder J, Pawson T, Klein R. 1996. Nuk controls pathfinding of commissural axons in the mammalian central nervous system. Cell 86:35–46.

Himanen JP, Chumley MJ, Lackmann M, Li C, Barton WA, Jeffrey PD, Vearing C, et al. 2004. Repelling class discrimination: Ephrin-A5 binds to and activates EphB2 receptor signaling. Nat Neurosci 7:501–509.

Hindges R, McLaughlin T, Genoud N, Henkemeyer M, O'Leary DD. 2002. EphB forward signaling controls directional branch extension and arborization required for dorsal-ventral retinotopic mapping. Neuron 35:475–487.

Holland SJ, Gale NW, Mbamalu G, Yancopoulos GD, Henkemeyer M, Pawson T. 1996. Bidirectional signalling through the EPH-family receptor Nuk and its transmembrane ligands. Nature 383:722–725.

Huberman AD, Murray KD, Warland DK, Feldheim DA, Chapman B. 2005. Ephrin-As mediate targeting of eye-specific projections to the lateral geniculate nucleus. Nat Neurosci 8:1013–1021.

Jackson H, Hackett JT, Rubel EW. 1982. Organization and development of brain stem auditory nuclei in the chick: Ontogeny of postsynaptic responses. J Comp Neurol 210:80–86.

Kania A, Jessell TM. 2003. Topographic motor projections in the limb imposed by LIM homeodomain protein regulation of ephrin-A–EphA interactions. Neuron 38:581–596.

Kim G, Kandler K. 2003. Elimination and strengthening of glycinergic/GABAergic connections during tonotopic map formation. Nat Neurosci 6:282–290.

Knoll B, Drescher U. 2002. Ephrin-As as receptors in topographic projections. Trends Neurosci 25:145–149.

Kullander K, Klein R. 2002. Mechanisms and functions of Eph and ephrin signalling. Nat Rev Mol Cell Biol 3:475–486.

Leake PA, Snyder RL, Hradek GT. 2002. Postnatal refinement of auditory nerve projections to the cochlear nucleus in cats. J Comp Neurol 448:6–27.

Lemke G, Reber M. 2005. Retinotectal mapping: New insights from molecular genetics. Annu Rev Cell Dev Biol 21:551–580.

Lippe W, Rubel EW. 1985. Ontogeny of tonotopic organization of brain stem auditory nuclei in the chicken: Implications for development of the place principle. J Comp Neurol 237:273–289.

Lyckman AW, Jhaveri S, Feldheim DA, Vanderhaeghen P, Flanagan JG, Sur M. 2001. Enhanced plasticity of retinothalamic projections in an ephrin-A2/A5 double mutant. J Neurosci 21:7684–7690.

Mann F, Harris WA, Holt CE. 2004. New views on retinal axon development: A navigation guide. Int J Dev Biol 48:957–964.

Mann F, Ray S, Harris W, Holt C. 2002. Topographic mapping in dorsoventral axis of the Xenopus retinotectal system depends on signaling through ephrin-B ligands. Neuron 35:461–473.

Marin O, Blanco MJ, Nieto MA. 2001. Differential expression of Eph receptors and ephrins correlates with the formation of topographic projections in primary and secondary visual circuits of the embryonic chick forebrain. Dev Biol 234:289–303.

McLaughlin T, Hindges R, Yates PA, O'Leary DD. 2003. Bifunctional action of ephrin-B1 as a repellent and attractant to control bidirectional branch extension in dorsal-ventral retinotopic mapping. Development 130: 2407–2418.

McLaughlin T, O'Leary DD. 2005. Molecular gradients and development of retinotopic maps. Annu Rev Neurosci 28:327–355.

Molea D, Rubel EW. 2003. Timing and topography of nucleus magnocellularis innervation by the cochlear ganglion. J Comp Neurol 466:577–591.

Momose-Sato Y, Glover JC, Sato K. 2006. Development of functional synaptic connections in the auditory system visualized with optical recording: Afferent-evoked activity is present from early stages. J Neurophysiol 96:1949–1962.

Nakamoto M, Cheng HJ, Friedman GC, McLaughlin T, Hansen MJ, Yoon CH, O'Leary DD, et al. 1996. Topographically specific effects of ELF-1 on retinal axon guidance in vitro and retinal axon mapping in vivo. Cell 86:755–766.

Pasquale EB. 2005. Eph receptor signalling casts a wide net on cell behaviour. Nat Rev Mol Cell Biol 6:462–475.

Person AL, Cerretti DP, Pasquale EB, Rubel EW, Cramer KS. 2004. Tonotopic gradients of Eph family proteins in the chick nucleus laminaris during synaptogenesis. J Neurobiol 60:28–39.

Pfeiffenberger C, Cutforth T, Woods G, Yamada J, Renteria RC, Copenhagen DR, Flanagan JG, et al. 2005. Ephrin-As and neural activity are required for eye-specific patterning during retinogeniculate mapping. Nat Neurosci 8:1022–1027.

Prakash N, Vanderhaeghen P, Cohen-Cory S, Frisen J, Flanagan JG, Frostig RD. 2000. Malformation of the functional organization of somatosensory cortex in adult ephrin-A5 knock-out mice revealed by in vivo functional imaging. J Neurosci 20:5841–5847.

Reber M, Burrola P, Lemke G. 2004. A relative signalling model for the formation of a topographic neural map. Nature 431:847–853.

Rubel EW, Fritzsch B. 2002. Auditory system development: Primary auditory neurons and their targets. Annu Rev Neurosci 25:51–101.

Rubel EW, Parks TN. 1975. Organization and development of brain stem auditory nuclei of the chicken: Tonotopic organization of n. magnocellularis and n. laminaris. J Comp Neurol 164:411–433.

Ryals BM, Rubel EW. 1982. Patterns of hair cell loss in chick basilar papilla after intense auditory stimulation. Frequency organization. Acta Otolaryngol 93: 205–210.

Sanes DH, Takacs C. 1993. Activity-dependent refinement of inhibitory connections. Eur J Neurosci 5:570–574.

Saunders JC, Coles RB, Gates GR. 1973. The development of auditory evoked responses in the cochlea and cochlear nuclei of the chick. Brain Res 63:59–74.

Siddiqui SA, Cramer KS. 2005. Differential expression of Eph receptors and ephrins in the cochlear ganglion and eighth cranial nerve of the chick embryo. J Comp Neurol 482:309–319.

Snyder RL, Leake PA. 1997. Topography of spiral ganglion projections to cochlear nucleus during postnatal development in cats. J Comp Neurol 384:293–311.

St John JA, Pasquale EB, Key B. 2002. EphA receptors and ephrin-A ligands exhibit highly regulated spatial and temporal expression patterns in the developing olfactory system. Brain Res Dev Brain Res 138:1–14.

Vanderhaeghen P, Lu Q, Prakash N, Frisen J, Walsh CA, Frostig RD, Flanagan JG. 2000. A mapping label required for normal scale of body representation in the cortex. Nat Neurosci 3:358–365.

Yates PA, Roskies AL, McLaughlin T, O'Leary DD. 2001. Topographic-specific axon branching controlled by ephrin-As is the critical event in retinotectal map development. J Neurosci 21:8548–8563.

Young SR, Rubel EW. 1983. Frequency-specific projections of individual neurons in chick brainstem auditory nuclei. J Neurosci 3:1373–1378.

Young SR, Rubel EW. 1986. Embryogenesis of arborization pattern and topography of individual axons in N. laminaris of the chicken brain stem. J Comp Neurol 254:425–459.

Yue Y, Chen ZY, Gale NW, Blair-Flynn J, Hu TJ, Yue X, Cooper M, et al. 2002. Mistargeting hippocampal axons by expression of a truncated Eph receptor. Proc Natl Acad Sci USA 99:10777–10782.

Zhang JH, Cerretti DP, Yu T, Flanagan JG, Zhou R. 1996. Detection of ligands in regions anatomically connected to neurons expressing the Eph receptor Bsk: Potential roles in neuron-target interaction. J Neurosci 16:7182–7192.

Zhang LI, Bao S, Merzenich MM. 2002. Disruption of primary auditory cortex by synchronous auditory inputs during a critical period. Proc Natl Acad Sci USA 99: 2309–2314.